

19. DATA REPORT: LATE PLEISTOCENE TERRIGENOUS INPUT TO SHATSKY RISE, SITE 1208¹

Susanne Gylesjö²

INTRODUCTION

Ocean Drilling Program Leg 198 Site 1208 is located on the Central High of Shatsky Rise ($36^{\circ}7.6301'N$, $158^{\circ}12.0952'E$) in the North Pacific Ocean at a water depth of 3346 m. A total of 345.9 m of sediment was recovered from Hole 1208A. The sediment was divided into two major stratigraphic units: Holocene–Paleocene alternating nannofossil clay and nannofossil ooze with diatoms and radiolarians (Unit I, Subunits IA, IB, and IC) and Campanian–Albian nannofossil ooze with minor chert (Unit II). This study reports the terrigenous contribution to Site 1208 for the upper 24 m of Subunit IA, corresponding to ~560 k.y.

METHODS

Terrigenous input was analyzed at sample intervals of ~20 cm, from 0 to 23.6 meters below seafloor (mbsf), yielding an age resolution of ~4.5 k.y. Bulk samples were freeze-dried, and ~5 g of each sample was weighed for analysis. To extract the terrigenous component of the sediments, the samples were first treated with 25% acetic acid solution buffered with sodium acetate to dissolve calcium carbonate. Iron oxides were removed using an oxalic acid reagent consisting of 0.2-M oxalic acid and 0.2-M ammonium oxalate. To dissolve biogenic silica, a 0.4-M sodium carbonate solution was used. After the chemical removals, the samples were freeze-dried and weighed. The extraction procedures used do not remove volcanic ash. There was only one sample collected from an interval where an ash layer was visible, but other samples may con-

¹Gylesjö, S., 2005. Data report: Late Pleistocene terrigenous input to Shatsky Rise, Site 1208. In Bralower, T.J., Premoli Silva, I., and Malone, M.J. (Eds.), *Proc. ODP, Sci. Results*, 198, 1–7 [Online]. Available from World Wide Web: <http://www-odp.tamu.edu/publications/198_SR/VOLUME/CHAPTERS/105.PDF>. [Cited YYYY-MM-DD]

²Geology and Geochemistry, Stockholm University, S-10691 Stockholm, Sweden.

susanne.gylesjo@geo.su.se

tain small amounts (<5%) of disseminated ash, as estimated from shipboard smear slide observations.

The mass accumulation rate (MAR) is a product of the linear sedimentation rate (LSR) and the dry bulk density (DBD) of the sample. The average LSR used for the MAR calculations is 4.24 cm/k.y. for the studied interval based on shipboard biostratigraphy, although the LSR between tie-points varies between 2.4 and 6.8 cm/k.y. The DBD was calculated by interpolating between shipboard physical property measurements, measured every ~1.5 m. The terrigenous flux is the product of the total MAR and the extracted fraction:

$$\text{Terrigenous MAR} = \text{fraction extracted} \times \text{LSR} \times \text{DBD},$$

where

MAR is given in g/cm²/k.y.,

LSR is given in cm/k.y., and

DBD is given in g/cm³.

No replicates of the extracted fraction were analyzed, but the uncertainties of the measured fraction contents are likely smaller than the uncertainties of the average LSR used for the MAR calculations.

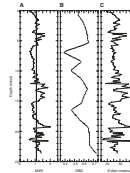
RESULTS

Figure F1 illustrates the eolian mass accumulation rate variation plotted vs. depth for the uppermost 24 m at Site 1208 (Table T1). The eolian MAR exhibits high variability from the bottom of the studied interval to ~18 mbsf. The eolian flux reaches the highest value (~2 g/cm²/k.y.) of the entire interval studied at 19.3 mbsf, after which it decreases uphole to ~0.75 g/cm²/k.y. at 15 mbsf. The interval between 18 and 15 mbsf has low eolian MAR and the variability is small. From 15 to 11–12 mbsf, the eolian MAR variability is high, ranging from 0.75 to 2 g/cm²/k.y. The eolian MAR exhibits ~1 g/cm²/k.y. decrease uphole from ~11 to 7 mbsf, and the variability is lower than that of the previous interval. The flux begins to increase again and shows higher variability between 6 and 3.5 mbsf, after which both the flux and the variability decrease toward the topmost sediments.

SUMMARY

The eolian mass accumulation rate at Site 1208 displays intervals of high-average MARs and high variability alternating with intervals of low-average MARs and low variability. The intervals with larger variation and higher-average eolian flux exhibit a somewhat cyclic pattern. The eolian MARs do not show a prominent increasing trend uphole, which would be expected and consistent with the trend of aridification of Asia over the last 500 k.y., and the intervals with high MAR and high variability do not seem to correspond to glacials, as expected. However, the ages in this study are based on an average linear sedimentation rate. The LSR, which is higher than that of typical pelagic sedimentation in this interval together with the seismic character suggests that the upper part of Site 1208 could be a drift deposit formed by bottom-current redistribution. Thus, there is most likely a problem with the ages used in

F1. MAR, DBD, and eolian material vs. depth, p. 5.



T1. Sediment data, p. 6.

this study. A visual comparison with a study by Hovan and Rea (1991) of eolian MAR from the same area and where $\delta^{18}\text{O}$ records are available shows similar patterns in some intervals and suggests that the ages in this study need to be improved. Generally, high-variability and high-MAR intervals are condensed in our study, whereas the low-variability and low-MAR intervals seem to be expanded compared to the study by Hovan and Rea (1991). This suggests that we have LSRs that are too low in the high-MAR intervals (glacials) and LSRs that are too high in the low-MAR intervals.

ACKNOWLEDGMENTS

This research used samples and/or data provided by the Ocean Drilling Program (ODP). ODP is sponsored by the U.S. National Science Foundation (NSF) and participating countries under management of Joint Oceanographic Institutions (JOI), Inc. Susanne Gylesjö was supported by a grant from the Swedish Natural Science Research Council for this study. Anna Neubeck and Natalja Eriksson assisted in the processing of the sediments.

REFERENCES

- Hovan, S.A., and Rea, D.K., 1991. Late Pleistocene continental climate and oceanic variability recorded in northwest Pacific sediments. *Paleoceanography*, 6(3):349–370.

Figure F1. A. Eolian mass accumulation rate (MAR). Black line = overall average MAR. B. Dry bulk density (DBD) plotted vs. depth. C. Percentage eolian material plotted vs. depth.

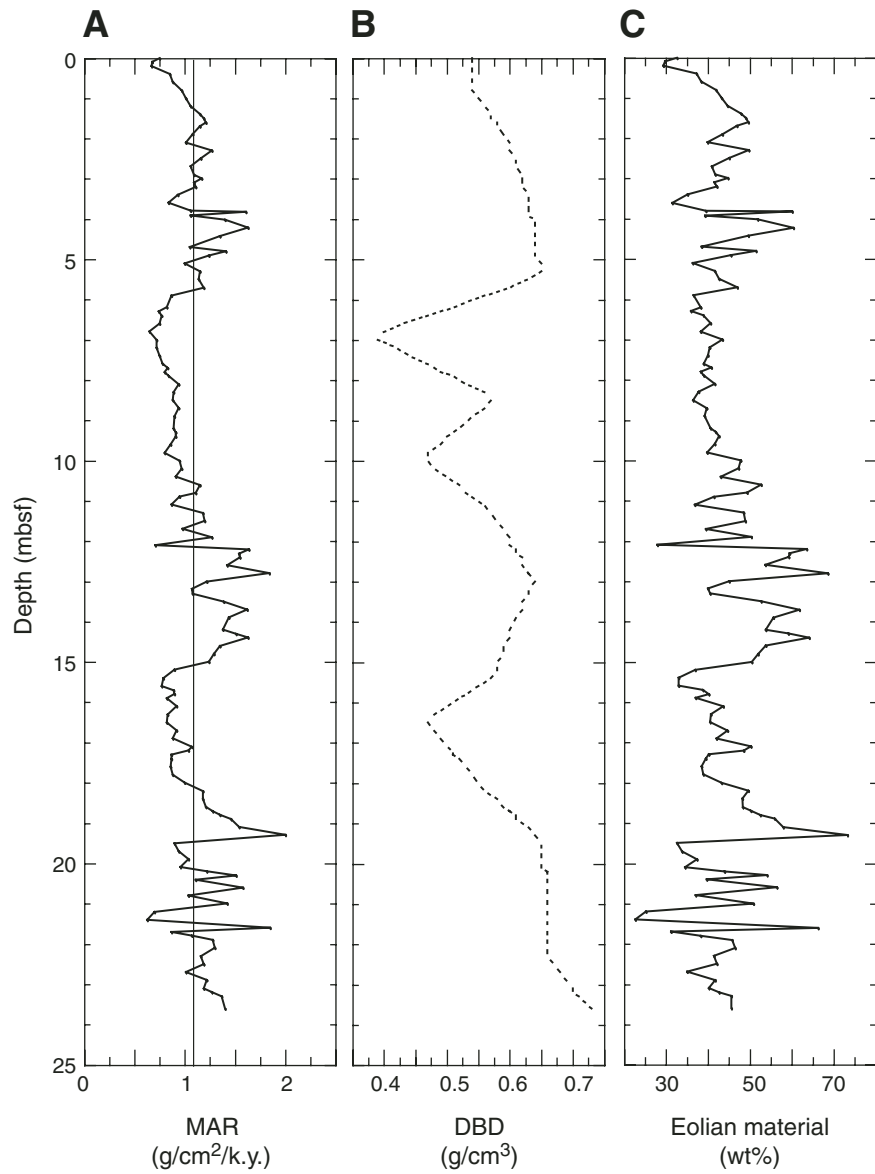


Table T1. Sediment data. (See table note. Continued on next page.)

Core, section, interval (cm)	Depth (mbsf)	Age (ka)	LSR	DBD (g/cm ³)	Eolian (wt%)	Eolian MAR (g/cm ² /k.y.)
198-1208A-						
1H-1, 0–2	0.00	0.2	4.24	0.54	32.60	0.75
1H-1, 10–12	0.10	2.6	4.24	0.54	29.76	0.68
1H-1, 20–22	0.20	5.0	4.24	0.54	29.38	0.67
1H-1, 40–42	0.40	9.7	4.24	0.54	37.30	0.85
1H-1, 60–62	0.60	14.4	4.24	0.54	38.35	0.88
1H-1, 80–82	0.80	19.1	4.24	0.54	41.99	0.97
1H-1, 100–102	1.00	23.8	4.24	0.55	43.23	1.01
1H-1, 120–122	1.20	28.5	4.24	0.56	44.64	1.06
1H-1, 140–142	1.40	33.3	4.24	0.57	47.88	1.15
1H-2, 0–2	1.50	35.6	4.24	0.57	49.00	1.19
1H-2, 10–12	1.60	38.0	4.24	0.58	49.64	1.21
1H-2, 20–22	1.70	40.3	4.24	0.58	46.88	1.15
1H-2, 40–42	1.90	45.0	4.24	0.59	43.44	1.08
1H-2, 60–62	2.10	49.8	4.24	0.60	39.92	1.01
1H-2, 80–82	2.30	54.5	4.24	0.60	49.79	1.27
1H-2, 100–102	2.50	59.2	4.24	0.61	45.11	1.16
1H-2, 120–122	2.70	63.9	4.24	0.61	40.92	1.06
1H-2, 140–142	2.90	68.6	4.24	0.62	41.73	1.09
1H-3, 0–2	3.00	71.0	4.24	0.62	44.75	1.17
1H-3, 10–12	3.10	73.3	4.24	0.62	41.55	1.09
1H-3, 20–22	3.20	75.7	4.24	0.62	42.15	1.11
1H-3, 40–42	3.40	80.4	4.24	0.63	35.17	0.93
1H-3, 60–62	3.60	85.1	4.24	0.63	31.51	0.84
1H-3, 80–82	3.80	89.9	4.24	0.63	39.54	1.06
1H-4, 0–2	3.82	90.3	4.24	0.63	60.08	1.61
1H-4, 10–12	3.92	92.7	4.24	0.63	39.28	1.06
1H-4, 20–22	4.02	95.0	4.24	0.64	51.86	1.40
1H-4, 40–42	4.22	99.8	4.24	0.64	60.36	1.63
1H-4, 60–62	4.42	104.5	4.24	0.64	49.66	1.35
2H-1, 0–2	4.70	111.1	4.24	0.64	38.54	1.05
2H-1, 10–12	4.80	113.4	4.24	0.64	51.51	1.41
2H-1, 20–22	4.90	115.8	4.24	0.64	45.54	1.24
2H-1, 40–42	5.10	120.5	4.24	0.65	36.41	1.00
2H-1, 60–62	5.30	125.2	4.24	0.65	41.66	1.15
2H-1, 80–82	5.50	130.0	4.24	0.63	42.68	1.14
2H-1, 100–102	5.70	134.7	4.24	0.60	47.02	1.19
2H-1, 120–122	5.90	139.4	4.24	0.56	36.53	0.87
2H-2, 0–2	6.20	146.5	4.24	0.51	38.25	0.82
2H-2, 10–12	6.30	148.8	4.24	0.49	35.98	0.74
2H-2, 20–22	6.40	151.2	4.24	0.47	38.88	0.77
2H-2, 40–42	6.60	155.9	4.24	0.43	40.67	0.75
2H-2, 60–62	6.80	160.6	4.24	0.40	38.32	0.65
2H-2, 80–82	7.00	165.3	4.24	0.39	43.48	0.72
2H-2, 100–102	7.20	170.0	4.24	0.42	40.43	0.72
2H-2, 120–122	7.40	174.8	4.24	0.44	40.00	0.75
2H-2, 140–142	7.60	179.5	4.24	0.47	38.99	0.78
2H-3, 0–2	7.70	181.8	4.24	0.48	40.85	0.83
2H-3, 10–12	7.80	184.2	4.24	0.49	38.29	0.80
2H-3, 20–22	7.90	186.6	4.24	0.51	39.00	0.84
2H-3, 40–42	8.10	191.3	4.24	0.53	41.59	0.94
2H-3, 60–62	8.30	196.0	4.24	0.56	37.81	0.89
2H-3, 80–82	8.50	200.7	4.24	0.57	36.47	0.88
2H-3, 100–102	8.70	205.4	4.24	0.56	39.73	0.94
2H-3, 120–122	8.90	210.1	4.24	0.54	39.18	0.90
2H-4, 0–2	9.20	217.2	4.24	0.52	40.61	0.89
2H-4, 10–12	9.30	219.6	4.24	0.51	41.80	0.91
2H-4, 20–22	9.40	221.9	4.24	0.50	42.60	0.91
2H-4, 40–42	9.60	226.7	4.24	0.49	41.65	0.86
2H-4, 60–62	9.80	231.4	4.24	0.47	39.84	0.80
2H-4, 80–82	10.00	236.1	4.24	0.47	47.78	0.95
2H-4, 100–102	10.20	240.8	4.24	0.48	47.28	0.97
2H-4, 120–122	10.40	245.5	4.24	0.50	43.08	0.91
2H-4, 140–142	10.60	250.2	4.24	0.52	52.72	1.15
2H-5, 10–12	10.80	255.0	4.24	0.53	49.29	1.11
2H-5, 20–22	10.90	257.3	4.24	0.54	41.39	0.95
2H-5, 40–42	11.10	262.0	4.24	0.56	36.88	0.87
2H-5, 60–62	11.30	266.7	4.24	0.57	48.48	1.18
2H-5, 80–82	11.50	271.5	4.24	0.58	48.98	1.20
2H-5, 100–102	11.70	276.2	4.24	0.59	39.49	0.98

Table T1 (continued).

Core, section, interval (cm)	Depth (mbsf)	Age (ka)	LSR	DBD (g/cm ³)	Eolian (wt%)	Eolian MAR (g/cm ² /k.y.)
2H-5, 120–122	11.90	280.9	4.24	0.60	50.33	1.27
2H-5, 140–142	12.10	285.6	4.24	0.60	27.94	0.71
2H-6, 0–2	12.20	288.0	4.24	0.61	63.50	1.64
2H-6, 11–13?	12.31	290.6	4.24	0.61	59.50	1.54
2H-6, 20–22	12.40	292.7	4.24	0.62	59.32	1.55
2H-6, 40–42	12.60	297.4	4.24	0.62	53.65	1.42
2H-6, 60–62	12.80	302.1	4.24	0.63	68.64	1.84
2H-6, 80–82	13.00	306.8	4.24	0.64	45.12	1.22
2H-6, 98–100	13.18	311.1	4.24	0.63	40.01	1.07
2H-7, 0–2	13.30	313.9	4.24	0.63	40.49	1.08
2H-7, 20–22	13.50	316.3	4.24	0.62	52.73	1.39
2H-7, 40–42	13.70	321.0	4.24	0.62	61.77	1.62
2H-7, 60–62	13.90	325.7	4.24	0.61	55.57	1.44
3H-1, 0–2	14.20	335.1	4.24	0.60	53.79	1.38
3H-1, 10–12	14.30	337.5	4.24	0.60	59.17	1.51
3H-1, 20–22	14.40	339.9	4.24	0.60	64.10	1.63
3H-1, 40–42	14.60	344.6	4.24	0.59	53.78	1.35
3H-1, 60–62	14.80	349.3	4.24	0.59	51.92	1.29
3H-1, 80–82	15.00	354.0	4.24	0.58	50.52	1.24
3H-1, 100–102	15.20	358.7	4.24	0.58	37.03	0.90
3H-1, 120–122	15.40	363.4	4.24	0.57	32.98	0.79
3H-1, 140–142	15.60	368.2	4.24	0.55	32.97	0.77
3H-2, 0–2	15.70	370.5	4.24	0.54	38.76	0.89
3H-2, 10–12	15.80	372.9	4.24	0.53	40.23	0.90
3H-2, 20–22	15.90	375.2	4.24	0.52	37.09	0.82
3H-2, 40–42	16.10	380.0	4.24	0.50	43.67	0.92
3H-2, 60–62	16.30	384.7	4.24	0.48	40.68	0.83
3H-2, 80–82	16.50	389.4	4.24	0.47	40.51	0.82
3H-2, 100–102	16.70	394.1	4.24	0.48	44.67	0.92
3H-2, 120–122	16.90	398.8	4.24	0.49	42.07	0.88
3H-2, 140–142	17.10	403.5	4.24	0.50	50.25	1.07
3H-3, 0–2	17.20	405.9	4.24	0.51	48.48	1.04
3H-3, 10–12	17.30	408.3	4.24	0.51	40.26	0.87
3H-3, 20–22	17.40	410.6	4.24	0.52	39.56	0.87
3H-3, 40–42	17.60	415.3	4.24	0.53	38.43	0.86
3H-3, 60–62	17.80	420.0	4.24	0.54	38.91	0.88
3H-3, 80–82	18.00	424.8	4.24	0.55	43.29	1.00
3H-3, 100–102	18.20	429.5	4.24	0.56	49.60	1.18
3H-3, 120–122	18.40	434.2	4.24	0.58	48.26	1.18
3H-3, 140–142	18.60	438.9	4.24	0.59	48.31	1.21
3H-4, 0–2	18.70	441.3	4.24	0.60	50.26	1.28
3H-4, 10–12	18.80	443.6	4.24	0.61	52.52	1.35
3H-4, 20–22	18.90	446.0	4.24	0.61	55.98	1.46
3H-4, 40–42	19.10	450.7	4.24	0.63	57.92	1.54
3H-4, 60–62	19.30	455.4	4.24	0.64	73.30	2.00
3H-4, 80–82	19.50	460.1	4.24	0.65	32.67	0.90
3H-4, 100–102	19.70	464.9	4.24	0.65	33.85	0.94
3H-4, 120–122	19.90	469.6	4.24	0.65	37.42	1.04
3H-4, 140–142	20.10	474.3	4.24	0.65	34.53	0.96
3H-5, 0–2	20.20	476.7	4.24	0.66	44.01	1.22
3H-5, 10–12	20.30	479.0	4.24	0.66	54.14	1.51
3H-5, 20–22	20.40	481.4	4.24	0.66	39.74	1.11
3H-5, 40–42	20.60	486.1	4.24	0.66	56.46	1.58
3H-5, 60–62	20.80	490.8	4.24	0.66	37.05	1.04
3H-5, 80–82	21.00	495.5	4.24	0.66	50.89	1.42
3H-5, 100–102	21.20	500.2	4.24	0.66	25.18	0.70
3H-5, 120–122	21.40	505.0	4.24	0.66	22.68	0.63
3H-5, 140–142	21.60	509.7	4.24	0.66	66.27	1.85
3H-6, 0–2	21.70	512.0	4.24	0.66	31.20	0.87
3H-6, 10–12	21.80	514.4	4.24	0.66	38.24	1.07
3H-6, 20–22	21.90	516.7	4.24	0.66	45.81	1.28
3H-6, 40–42	22.10	521.5	4.24	0.66	46.49	1.30
3H-6, 60–62	22.30	526.2	4.24	0.66	41.46	1.16
3H-6, 80–82	22.50	530.9	4.24	0.67	42.17	1.19
3H-6, 100–102	22.70	535.6	4.24	0.68	35.05	1.01
3H-6, 120–122	22.90	540.3	4.24	0.69	41.75	1.22
3H-6, 140–142	23.10	545.0	4.24	0.70	40.19	1.19
3H-7, 0–2	23.20	547.4	4.24	0.70	42.59	1.27
3H-7, 10–12	23.30	549.8	4.24	0.71	45.63	1.37
3H-7, 40–42	23.60	556.8	4.24	0.73	45.60	1.40

Note: DBD = dry bulk density, LSR = linear sedimentation rate, MAR = mass accumulation rate.